Author's Accepted Manuscript

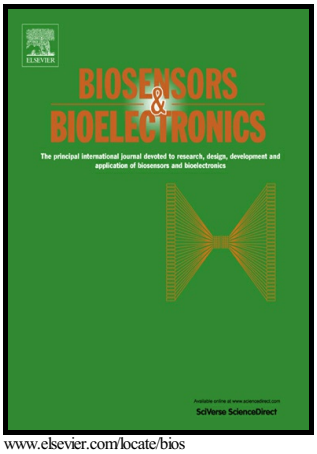

www.elsevier.com/locate/bios

An enzyme-free and label-free surface plasmon resonance biosensor for ultrasensitive detection of fusion gene based on DNA self-assembly hydrogel with streptavidin encapsulation

Bin Guo, Bo Wen, Wei Cheng, Xiaoyan Zhou, Xiaolei Duan, Min Zhao, Qianfeng Xia, Shijia Ding

PII: S0956-5663(18)30287-2
DOI: https://doi.org/10.1016/j.bios.2018.04.027
Reference: BIOS10423

To appear in: *Biosensors and Bioelectronic*

Received date: 13 January 2018
Accepted date: 13 April 2018

Cite this article as: Bin Guo, Bo Wen, Wei Cheng, Xiaoyan Zhou, Xiaolei Duan, Min Zhao, Qianfeng Xia and Shijia Ding, An enzyme-free and label-free surface plasmon resonance biosensor for ultrasensitive detection of fusion gene based on DNA self-assembly hydrogel with streptavidin encapsulation, *Biosensors and Bioelectronic,* https://doi.org/10.1016/j.bios.2018.04.027

An enzyme-free and label-free surface plasmon resonance biosensor for ultrasensitive detection of fusion gene based on DNA self-assembly hydrogel with streptavidin encapsulation

Bin Guo[a,d,1], Bo Wen[a,1], Wei Cheng[b], Xiaoyan Zhou[a], Xiaolei Duan[a], Min Zhao[a], Qianfeng Xia[c,*], Shijia Ding[a,*]

[a]*Key Laboratory of Clinical Laboratory Diagnostics (Ministry of Education), College of Laboratory Medicine, Chongqing Medical University, Chongqing 400016, China*

[b]*The Center for Clinical Molecular Medical Detection, The First Affiliated Hospital of Chongqing Medical University, Chongqing 400016, China*

[c]*Laboratory of Tropical Biomedicine and Biotechnology, Faculty of Tropical Biomedicine and Laboratory Medicine, Hainan medical University, Haikou, Hainan 571101, China*

[d] *Department of Clinical Laboratory, The Affiliated Hospital of North Sichuan Medical College, Nanchong 637000, China*

**Corresponding author: Tel: +86-23-68485688, Fax: +86-23-68485786. E-mail address: dingshijia@163.com (S.J. Ding)*

[1]*These authors contributed equally to this work.*

Abstract

In this research, an enzyme-free and label-free surface plasmon resonance (SPR) biosensing strategy has been developed for ultrasensitive detection of fusion gene based on the heterogeneous target-triggered DNA self-assembly aptamer-based hydrogel with streptavidin (SA) encapsulation. In the presence of target, the capture probes (Cp) immobilized on the chip surface can capture the PML/RARα, forming a Cp-PML/RARα duplex. After that, the aptamer-based network hydrogel nanostructure is formed on the gold surface via target-triggered self-assembly of X shaped polymers. Subsequently, the SA can be encapsulated into hydrogel by the specific binding of SA aptamer, forming the complex with super molecular weight. Thus, the developed strategy achieves dramatic enhancement of the SPR signal. Using PML/RARα "S" subtype as model analyte, the developed biosensing method can detect target down to 45.22 fM with a wide linear range from 100 fM to10 nM. Moreover, the high efficiency biosensing method shows excellent practical ability to identify the clinical PCR products of PML/RARα. Thus, this proposed strategy presents a powerful platform for ultrasensitive detection of fusion gene and early diagnosis and monitoring of disease.

Keywords: Surface plasmon resonance; DNA self-assembly; Aptamer-based DNA hydrogel; Streptavidin aptamer; PML/RARα

1. Introduction

Surface plasmon resonance (SPR) is a real-time and label-free technique in clinical analysis for biomolecules (Nguyen et al., 2015). At present, the enhancement of the sensitivity of SPR is a challenge for its practical application due to inability to measure extreme small changes in refractive index (He et al., 2000). To improve sensitivity of SPR biosensor, different amplification strategies have been explored, including enzyme-amplified based strategies (He et al., 2014; Nawattanapaiboon et al., 2015), nanomaterial based strategies (Liu et al., 2017; Wang et al., 2016) and enzyme-free DNA self-assembly based strategies (Li et al., 2014). Among these strategies, enzyme-free DNA self-assemblies capable of constructing a variety of nanostructures have been widely explored due to flexible design, controllable size and orientation, ease of bioconjugation and excellent biocompatibility (Hu et al., 2011; Couvreur and Vauthier, 2006; Evans et al., 2016). For example, catalytic hairpin assembly (CHA) (Li et al., 2016a; Li et al., 2016b) and hybridization chain reaction (HCR) (Ding et al., 2017) strategies show certain amplified efficiency in biosensing assay, fulfilling the

picomole level detection of target DNA. However, one of the crucial challenges in fabrication of DNA self-assembly based SPR biosensors is still the limited signal enhancement efficiency.

DNA-based hydrogels, the two- or three-dimensional crosslinked network polymers containing over 90% of water, are the important biomaterials in bioanalysis and biomedicine owing to its high biocompatibility, high flexibility and highly tunable nature (Kouwer et al., 2013; Holtz and Asher, 1997). There are three types of DNA-based hydrogels, including DNA-hybrid, pure DNA-hybridization and physical interaction hydrogels. In particular, the pure DNA hydrogel, formed by crosslink of DNA building blocks via sequence-directed hybridization, receives extensive attention in recent years (Jones et al., 2015; Zhang et al., 2013a; Chou et al., 2014). For example, Xing et al. develop a novel pure DNA hydrogel by directly accumulating the Y-scaffold and the linker DNA, responding successfully to thermal and enzyme stimulus (Xing et al., 2011). The pure DNA hydrogel holds several remarkable features of stability, flexibility, precision, stimuli-responsive, facile synthesis and modification, which has potential application in biosensing (Li et al., 2016c).

Functional nucleic acids (FNAs), including aptamers (Mastronardi et al., 2014), DNAzymes (Teller and Willner, 2010), G-quadruplexes-motif structures (Xiang et al., 2016), can perform active roles in recognition, binding and catalysis of target (Sefah et al., 2009). Among these FNAs, aptamers have been regarded as promising recognition elements for biosensors due to very low cost, high stability, high reproducibility in target recognition and ease of labeling and chemical modification. Significant efforts have been devoted to the development of aptasensors using different transducers such as surface plasma resonance (Li et al., 2016b) and biolayer interferometry (Gao et al., 2017b), also significantly expanding the application field of hydrogels by responding to diversified stimuli such as proteins and nucleic acids. These methodology can be easily adapted for the detection of biomolecules in a rapid, sensitive and real-time manner (Gao et al., 2017a). At present, various aptamer-based DNA hydrogel biosensing strategies have been developed for detection of biomolecules, including adenosine-responsive biosensor (Yang et al., 2008), cocaine-responsive biosensor (Zhu et al., 2010; Yan et al., 2013) and protein-responsive biosensor (zhang et al., 2013b). In responsive process of the three biosensors, the

aptamers can specifically bind with the target to form target-aptamer complex, resulting in the breakdown of the hydrogel and achieving the specific detection of adenosine, cocaine and protein, respectively. Recently, Fan's group reported an aptamer-trigger clamped hybridization chain reaction (atcHCR) method for in situ identification and subsequent cloaking/decloaking of CTCs by porous DNA hydrogels, opening new powerful and effective routes for cancer diagnostics and therapeutics (Song et al., 2017). More importantly, aptamer-based DNA hydrogel can recognize and encapsulate macromolecular proteins with better sequence arrangement density and molecular weight, which can enhance significantly the SPR response signal depending on the formation of super molecular weight nanostructures bound to the gold surface. To date, few papers have reported the application of the aptamer-based network hydrogel nanostructure with protein encapsulation in SPR biosensor.

Herein, aiming at exploring highly efficient strategy for signal amplification, an enzyme-free and label-free SPR biosensing strategy has been developed for ultrasensitive detection of fusion gene based on DNA self-assembly aptamer-based hydrogel with streptavidin (SA) encapsulation. PML/RARα (promyelocytic leukemia, retinoic acid receptor alpha) is the product of the chromosomal translocation t (15; 17)(q22; q21) and specifically occurs in acute promyelocytic leukemia (De Thé et al., 1990; Chen and Chen, 1992). Efficient detection of the PML/RARα can provide the molecular basis for diagnosing and monitoring disease in APL patients. Therefore, using PML/RARα "S" subtype as a model target DNA, the developed method achieves ultrasensitive detection of PML/RARα with high specificity. Furthermore, the clinical PCR products of the PML/RARα have been successfully identified by the developed biosensing strategy. Thus, the proposed biosensor presents a pragmatic platform towards high efficient detection for a variety of fusion gene in clinical diagnosis.

2. Experiment section

2.1. Reagents and Materials

All oligonucleotides were synthesized by Sangon Inc. (Shanghai, China) and purified by high-performance liquid chromatography, and the base sequences were listed in Table S1 (Supporting information). All oligonucleotides were dissolved in hybridization buffer (pH 7.4) containing 30 mM sodium phosphate, 450 mM NaCl, 3

mM EDTA, 0.25% Triton 100, and stored at -20 °C. 6-Mercapto-1-hexanol (MCH), streptavidin and salmon sperm DNA were purchased from Sigma-Aldrich (St. Louis, MO, USA). DL1000 DNA Marker and agarose were purchased from TaKaRa Biotech (Dalian, China). RNA extraction Kit was purchased from Amoy Diagnostics (Xiamen, China). RT-PCR Kit was purchased from Yqbiomed (Shanghai, China). All other reagents were of analytical grade and without further purification. Ultrapure water from a Millipore water purification system (≥18 MΩ·cm, Milli-Q, Millipore) was used in all experiments.

2.2. Apparatus

The SPR Biacore X™ analytical system and the bare gold sensor chip (Biacore AB, Uppsala, Sweden) were used in experiments. A time course of resonance unit (RU) was employed to display the result. Sensorgram was generated from the RU trace and evaluated by fitting algorithms which compared the raw data to well-defined binding model. Cobas z analyzer was used for real-time fluorescent quantitative PCR (qPCR) (Roche, Switzerland). DYY-6C electrophoresis analyzer (Liuyi Instrument Company, China) and Bio-rad ChemDoc XRS (Bio-Rad, USA) were used for gel electrophoresis and imaging, respectively. Atomic force microscope (AFM) (Bruker AXS, Germany) was employed to characterize the size and morphology of DNA network hydrogel nanostructure.

2.3. Preparation of X shaped polymer and aptamer-based DNA hydrogel

Stock solutions of DNA strands X shaped polymer 1 (X1)-S1, S2, S3, S4 and X shaped polymer 2 (X2)-S1, S2, S3, S4 were prepared with concentration of 10 μM. The stock solution contained 30 mM sodium phosphate, 450 mM NaCl, 3 mM EDTA, 0.25% Triton 100, 10 μM DNA strand S1, S2, S3 or S4 and ultrapure water. After that, 10 μL of 10 μM four DNA strands (X1-S1, S2, S3, S4 or X2-S1, S2, S3, S4) were added into an Eppendorf (EP) tube with a 60 μL hybridization buffer solution to obtain a mixture of 1 μM concentration. Then, the mixture was annealed to form the desired two types of X shaped polymers using the following process: 95 °C, 5 min; 65 °C, 30 min; 50 °C, 30 min; 37 °C, 30 min; 20 °C, 30 min; and 4 °C, 24 h. After that, 100 μL solution containing X1 and 100 μL solution containing X2 were simply mixed and shaken well followed by hybridizing at room temperature for 60 min to form the aptamer-based DNA network hydrogel nanostructure.

2.4. Preparation of sensing chip

Firstly, the gold chip was cleaned with fresh piranha solution (H_2SO_4: H_2O_2=3:1) for 5 min to eliminate other substances, followed by rinsing thoroughly with Millipore-Q water and allowing to dry. The ready chip was docked in the Biacore X™ instrument socket and ran the sensorgram for 2 hours. Secondly, 1 μM thiolated capture probes (Cp) in immobilization solution (1 mM KH_2PO_4, pH 3.8) were injected into the flow-cell for 30 min. Thirdly, the resulting chip was further passivated with 1 mM MCH solution for 4 h at room temperature to reduce nonspecific binding of DNA on the chip surface. Finally, after washing with Millipore-Q water, the chip was left to dry and docked for further measurement.

2.5. Fabrication of SPR biosensor and PML/RARα analysis

100 μL PML/RARα DNA with various concentrations was added into the flow-cell and hybridized with the capture probes immobilized on the chip surface for 30 min. After that, the DNA network hydrogel nanostructure was formed by two steps. Firstly, 100 μL of 100 nM X1 was added into flow-cell and hybridized with the unpaired fragment of PML/RARα DNA for 30 min. Then, 100 μL mixture containing 100 nM X1 and 100 nM X2 was added into flow-cell for 30 min, forming the network hydrogel nanostructure by hybridization of the sticky ends on the chip surface. Finally, the solution of 650 nM SA in running buffer was injected and flowed through the flow-cell for 30 min. Hybridization buffer was used as the running buffer in the experiment. All hybridization reactions were carried out at a flow rate of 2 μL min^{-1}. Upon the above experiment process, the SPR biosensor was fabricated successfully for PML/RARα analysis. After each detection process, 5 μL of 50 mM NaOH was injected to remove the binding analytes on the gold film for the next detection. The target DNA was repeatedly measured by three times on the same chip and took the average value as the final result.

2.6. Gel electrophoresis

A 2% agarose gel electrophoresis analysis of self-assembly of the two types of X shaped polymers and the network hydrogel nanostructure was carried out in 1× TBE buffer (90 mM Tris–HCl, 90 mM boric acid, 2 mM EDTA, pH 7.4) at 120 mV for about 30 min. The gel was photographed by Bio-Rad digital.

2.7. Identification of PML/RARα in clinical samples

To further evaluate the clinical application, the developed biosensing method was used to analyze the denatured PCR amplification products of bone marrow samples from acute promyelocytic leukemia. All the PCR products were obtained from the First Affiliated Hospital of Chongqing Medical University. Firstly, total RNA was extracted from bone marrow samples by using TRIzol reagent. Then, to mix 8 μL reaction liquid (dNTPs, $MgCl_2$, Mixed enzyme buffer), 1 μL sense primer (10 pmol μL^{-1}), 1 μL antisense primer (10 pmol μL^{-1}) and 15 μL RNA sample into the reaction tube. The RT-PCR amplification protocol was as follows, 42°C for 30 min, 5 min at 94°C followed by 35 cycles of 94°C for 45 s, 61°C for 80 s, and 72°C for 30 s. The PCR products were characterized with 2% agarose gel electrophoresis. Then, all PCR products were diluted by 10 times with hybridization buffer, denatured by 5 min at 95°C and annealed by cooling in an ice-water for 5 min. Subsequently, SPR detections were performed following the same procedure used for synthetic DNA. After that, the PCR products were continuously diluted 10^2, 10^3, 10^4, 10^5, 10^6, 10^7 times for the SPR and qPCR detection.

3. Results and discussion

3.1. Design principle of the biosensor

An overview of the proposed SPR biosensor for detection of PML/RARα is illustrated in Scheme 1. As shown in Scheme 1A, two types of X shaped polymers are prepared firstly as the building blocks. The four DNA strands (S1, S2, S3 and S4) belonged to X1 or X2 are annealed to form the desired X shaped polymers by complementation of bases among four strands. The X shaped branched nanostructure contains two SA aptamers at 5'-ends for SA binding and four 20 bases of overhang arms at 3'-ends for hybridization of sticky ends between X1 and X2 to form the aptamer-based network hydrogel nanostructure. To control the precise self-assembly of network, the hybridization rule is formulated only to allow crosslink between X1-S1 and X2-S3, X1-S2 and X2-S4, X1-S3 and X2-S1, X1-S4 and X2-S2. As shown in Scheme 1B, the biosensing protocol of target DNA includes four steps. First, the capture probes immobilized on the chip surface hybridize with the PML/RARα used as linker, forming a Cp-PML/RARα duplex. Then, the exposing 20 bases of RARα fragment can specifically hybridize with the X1, resulting in formation of the

sandwich structure. With the additional introduction of X1 and X2, the aptamer-based network hydrogel nanostructure is formed via crosslink of two types of X shaped polymers on the chip surface. Subsequently, the SA aptamer incorporated into hydrogel can strongly bind SA to further amplify the response signal. Thus, the SPR signal is enhanced dramatically owing to the forming complex with super molecular weight. On the contrary, in the absence of the PML/RARα, the network hydrogel nanostructure exists only in homogeneous phase and almost negligible SPR signal is observed. Thus, the developed strategy achieves ultrasensitive detection of PML/RARα.

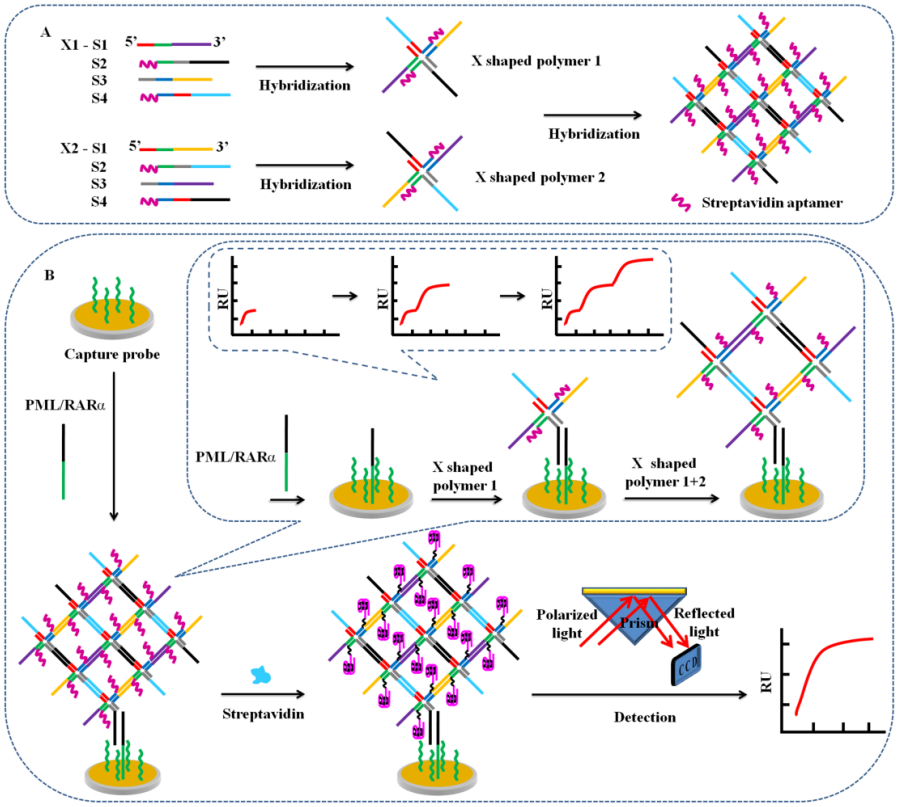

Scheme 1. Schematic illustration of the SPR biosensing strategy via heterogeneous fusion gene-triggered DNA self-assembly aptamer-based hydrogel with SA encapsulation for signal amplification and PML/RARα detection.

3.2. Characterization of X shaped polymer self-assembly

The conformation of X shaped polymer can be strongly influenced by the complementary base numbers among S1, S2, S3 and S4. If the crosslink parts are excessive short, it is difficult to form stable X shaped polymer. On the other hand, the crosslink parts of excessive long increase the chance of forming complex secondary

structure and synthetic cost of the sequences. Therefore, the numbers of different complementary base from 7 to 15 were investigated in this work. As shown in Fig. 1A, Lane 5, 6 showed the correct assembly products of X shaped polymers, corresponding base numbers were 13 and 15, respectively. As shown in Fig. 1B, the signal-to-noise ratio reached the peak and tended to stable as the increasing numbers of complementary base up to 13. Therefore, the 13 was selected as the optimal complementary base number among S1, S2, S3 and S4.

The assembly efficiency of X shaped polymer is highly sensitive to the annealing conditions. In this work, sufficient annealing time at 4 °C was needed to increase the assembly efficiency of X shaped polymer and reduce the competitive inhibition of network hydrogel nanostructure assembly. Hence, to obtain the best SPR response signal, different annealing time at 4 °C in the range from 1 to 48 hours was investigated in this work. As shown in Fig. S1, the SPR signal-to-noise ratio started to increase as the increasing time up to 24 hours. Then, the signal-to-noise ratio tended to stable. Thus, annealing time of 24 hours was chosen.

To confirm the stability of the effective X shaped polymer assembly, we evaluated the ΔRU of the X shaped polymer based on SPR measurement under five individual self-assembly. As shown in Table S2, the coefficient of variations was 1.08%. The result indicated that the self-assembly X shaped polymer was stable for signal output.

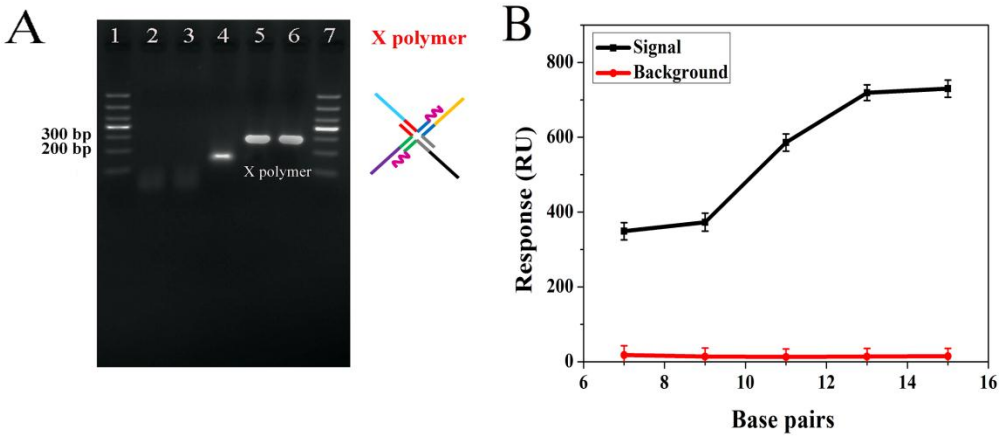

Fig. 1. (A) 2% agarose gel electrophoretic confirmation of X shaped polymers corresponding to different complementary base numbers among S1, S2, S3 and S4: Lane 1, 7: DL 1000 DNA ladder marker; Lane 2: 7 complementary bases; Lane 3: 9 complementary bases; Lane 4: 11 complementary bases; Lane 5: 13 complementary bases; Lane 6: 15 complementary bases. (B)

Characterization of SPR response signals for X shaped polymers corresponding to different complementary base numbers: 7, 9, 11, 13, 15 among S1, S2, S3 and S4. Error bar represents the standard deviation (n = 3).

3.3. Feasible analysis of the biosensing strategy

To confirm effective self-assembly of the network hydrogel nanostructure based on X shaped polymer, the hybridization reaction products of different chains were characterized by 2% agarose gel electrophoresis. As shown in Fig. 2A, as anticipated, with the hybridization of S1, S2, S3 and S4, the clear bands exhibited the efficient X1 assembly products (Lane 4) and X2 assembly products (Lane 7), respectively, indicating a well integration of four hybridization chains. The generated products of network hydrogel nanostructure gave the mobility corresponding to the 700-1000 base pair marker (Lane 8), much slower than that of the single X shaped polymers. These results demonstrated the programmed assembly work as expectation.

The formation of DNA hydrogel nanostructure was confirmed using AFM. Fig. 2B was a typical AFM image of DNA hydrogel nanostructure, which showed surface morphology of the network nanostructure with a mean diameter of 125.2 ± 7.5 nm and mean height of 4.15 ± 2.6 nm. The AFM visualization results reflected the formation of DNA network hydrogel nanostructure.

SPR experiments were performed to further confirm the validity of the amplification strategy. As shown in Fig. 2C, in the presence of PML/RARα, a mean response signal ΔRU1 of 156 RU was obtained by the formation of Cp-PML/RARα duplex. After introduction of the X1, the Cp-PML/RARα-X1 triplet enhanced the mean response signal ΔRU2 of 724 RU. A persistently increasing mean response signal ΔRU3 of 601 RU was obtained owing to higher molecular weight of the network hydrogel nanostructure assembled on the chip surface. Subsequently, the SA aptamer encapsulated the SA into hydrogel to further amplify the mean response signal ΔRU4 of 221 RU. The results demonstrated the remarkable signal amplification of the designed method for ultrasensitive target DNA detection.

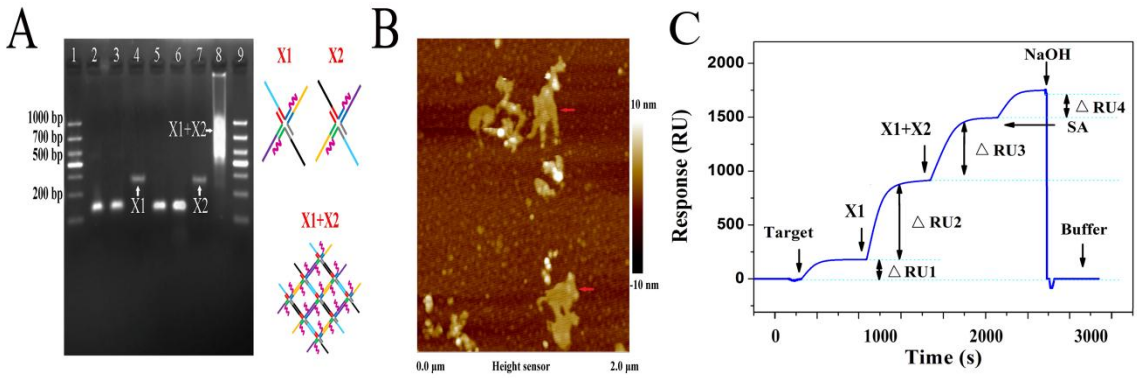

Fig. 2. (A) 2% agarose gel electrophoretic confirmation of X shaped polymer and network hydrogel nanostructure: Lane 1, 9: DL 1000 DNA ladder marker; Lane 2, 3 and 4: X1-(S1+S2), X1-(S1+S2+S3), X1-(S1+S2+S3+S4), respectively. Lane 5, 6 and 7: X2-(S1+S2), X2-(S1+S2+S3), X2-(S1+S2+S3+S4), respectively. Lane 8: X1-(S1+S2+S3+S4)+X2-(S1+S2+S3+S4). (B) AFM images of the network hydrogel nanostructure formed by X1+X2. (C) The diagram of SPR response signals for the hydrogel with SA encapsulation amplification strategy corresponding to consecutive introduction of PML/RARα (ΔRU1), X1 (ΔRU2), X1+X2 (ΔRU3) and SA (ΔRU4).

3.4. Optimization of experimental conditions

To enhance sensitivity of detection, three injection approaches for formation of network hydrogel nanostructure on the gold film were investigated in this work, including the injection approach by one step (simultaneous injection of target DNA, X1 and X2 into flow-cell for 60 min), the injection approach by two steps (injection of target DNA into flow-cell for 60 min, injection of X1 and X2 into flow-cell for 60 min) and the injection approach by three steps (injection of target DNA into flow-cell for 60 min, injection of X1 into flow-cell for 60 min, injection of X1 and X2 into flow-cell for 60 min). As shown in Fig. S2A, it was clear that the injection approach by three steps obtained the best signal-to-noise ratio due to the least competitive inhibition in hybridization process, which was chosen to further experiment.

To improve efficiency of detection, the reaction time after each injection was optimized. The reaction time of four injections was set to the same in this study. As shown in Fig. S2B, the data points (20, 30, 40, 50, 60) displayed in the abscissa represented 20, 30, 40, 50, 60 minutes reaction time after each injection. Thus the total reaction time after four steps was 80, 120, 160, 200, 240 minutes, respectively. The final signals after four injections were displayed in the ordinate. The signal-to-noise ratio ascended with the increase of reaction time. While the time of each

injection extended to 30 min, the signal-to-noise ratio reached the peak and tended to stable. Hence, 30 min was chosen as the optimal time of every step.

In addition, to further enhance the sensitivity, the concentration of SA was also optimized in the range from 250 nM to 750 nM. The result of optimization was depicted in Fig. S2C. The signal-to-noise ratio increased and then reached the maximum at 650 nM, suggesting that 650 nM was the optimal concentration of SA.

3.5. Analytical performance of the biosensor

Under optimal experimental conditions, the analytical performance of the biosensor for PML/RARα detection was investigated. As exhibited in Fig. 3B, the intensity of SPR signal increased upon the elevated PML/RARα DNA concentrations. The calibration plots showed a "S" relationship between the response signal and the logarithm of PML/RARα DNA concentrations in the range from 100 fM to 100 nM. As exhibited in Fig. 3A, the elevated PML/RARα DNA concentrations from 100 fM to10 nM led to a proportional SPR response signal increase. The inset of Fig. 3A exhibited the calibration plots of response signals *vs* the logarithm of PML/RARα DNA concentrations with a linear regression equation of Y=47.47×lg*c* (fM)-74.08 (where Y was the SPR response signal and c was the concentration of PML/RARα DNA) and a correlation coefficient of 0.9981. Moreover, the detection limit (LOD) estimated at 3σ was calculated to be 45.22 fM. The data was compared with those of reported SPR biosensing methods for the detection of DNA or RNA (Table S3) and different methods for the detection of PML/RARα (Table S4), demonstrating that this proposed method for PML/RARα analysis with better sensitivity, which was attributed to the powerful amplification of target-triggered DNA self-assembly hydrogel with SA encapsulation.

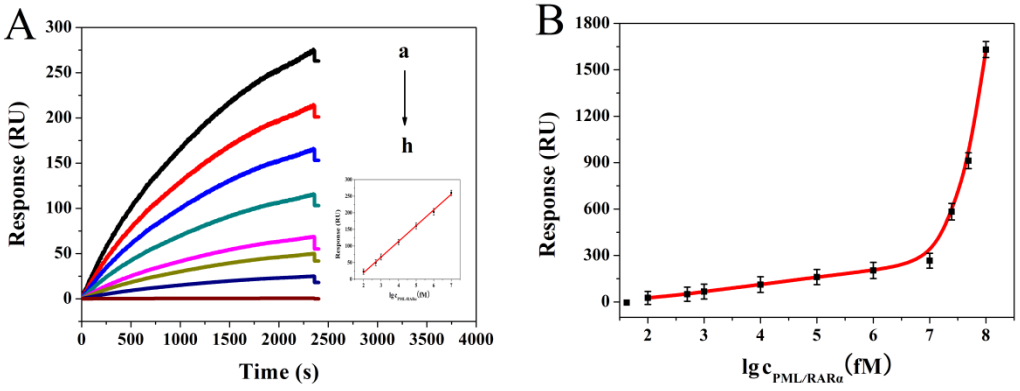

Fig. 3. (A) SPR sensorgrams for detection of PML/RARα at 1× 10^7, 1× 10^6, 1× 10^5, 1× 10^4, 1× 10^3, 500, 100 and 0 fM (from a to h) and the inset was the calibration plots of SPR response singnal vs the logarithm of PML/RARα concentrations from 100 fM to 10 nM. (B) The calibration curve of ΔRU versus PML/RARα DNA concentrations at 1× 10^8, 5× 10^7, 2.5× 10^7, 1× 10^7, 1× 10^6, 1× 10^5, 1× 10^4, 1× 10^3, 500, 100 and 0 fM. Error bar represents the standard deviation (n = 3).

3.6. Specificity, reproducibility and recovery for PML/RARα detection

To investigate the specificity of the proposed biosensor, the SPR response signals were compared by detecting "S" subtype PML/RARα DNA, PML DNA, RARα DNA, PML/RARα DNA of different subtypes ("L" and "V" subtypes) and hybridization buffer used as blank. As shown in Fig. 4, in the same concentration of DNA, the signal of PML/RARα DNA "S" subtype (curve a) was about 11 times of that of PML DNA (curve b). The signals had no significant difference with the blank (curve f) in the presence of RARα DNA (curve e), PML/RARα DNA "L" subtype (curve c) and "V" subtype (curve d). Therefore, these results indicated that the biosensor displayed excellent specificity due to the selective crosslink between Cp and complex with super molecular weight.

In addition, the same PML/RARα DNA samples had been measured five times to verify the reproducibility of intra- and inter-assay. As shown in Table S5, the coefficient of variation was 2.11% and the standard deviation (SD) was 4.33% for the intra-assay. And the coefficient of variation was 3.26% and the standard deviation (SD) was 6.73% for the inter-assay, demonstrating good fabrication reproducibility.

To assess the reliability and dependability of the developed method in complex biological environment, the recovery tests were performed using salmon sperm DNA. Samples of three different concentrations were prepared by mixing synthetic PML/RARα DNA with 1 mg mL^{-1} salmon sperm DNA. The recoveries were 115%, 96.3%, 105.2% respectively in 10 pM, 100 pM and 1000 pM (Table S6), indicating that the developed method could be a probable approach for target DNA analysis in complex biological sample.

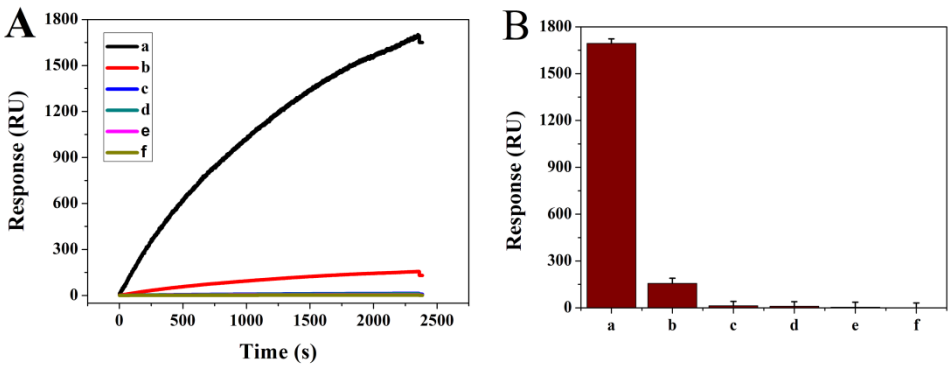

Fig. 4. (A) SPR sensorgrams and (B) SPR response signals for specificity of PML/RARα detection against PML/RARα DNA "S" subtype (a) and different non-targets: PML DNA (b), PML/RARα DNA "L" subtype (c), PML/RARα DNA "V" subtype (d), RARα DNA (e), blank (f). Error bar represents the standard deviation (n = 3).

3.7. Identification of PML/RARα in clinical samples

The denatured PML/RARα fragments after PCR amplification were assayed by the developed biosensor to evaluate the potential application. Fig. 5A showed the electrophoresis result of PCR products. The PCR products from the negative sample (Lane 3) and blank control (Lane 4) did not show any band in the gel. Obviously, the light band was observed in the gel with PCR products from positive sample (Lane 2). As shown in Fig. 5B, as anticipated, a great amplified SPR signal was obtained as detecting the positive PCR products (curve a), indicating the developed biosensor could recognize effectively target DNA via the specific capture. By contrast, the extreme small SPR signal was observed as detecting the negative PCR products (curve b). As shown in Fig. S3, the positive and negative PCR products gave a average value of 185 RU with the mean standard deviation (SD) of 7.71% and a average value of 13 RU with the mean SD of 5.29%, indicating that the method had great identification of the positive and negative PCR products. To further verify the detection accuracy of clinical samples by the developed biosensor, qPCR and SPR were used to measure the PCR products of different dilutions. As comparing the results of two assays using regression analysis, the plots of cycle thresholds (Ct) obtained with the qPCR assay *vs* those of SPR signals obtained with the developed biosensor showed a good linear relationship, with the correlation coefficient of 0.9976 (Fig. S4), confirming the good consistency of two methods. Therefore, practicality of the developed biosensor was further confirmed. However, the SPR signals of PCR

products were smaller than those of synthetic DNA (Fig. S5). This might be attributed to formation of secondary structure of long oligonucleotides, which interfered with efficiency of hybridization between target DNA and capture probe (Gao et al., 2006). Therefore, the detection of long oligonucleotides should be further studied.

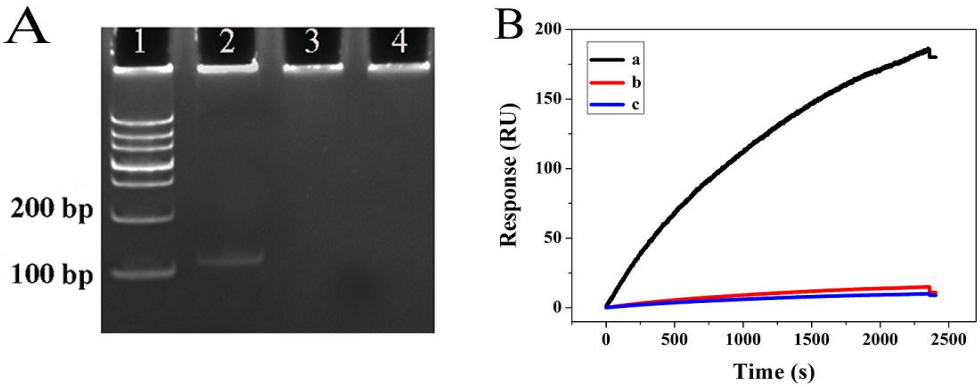

Fig. 5. (A) Electropherogram of PCR products: Lane 1: DL 1000 DNA ladder marker; Lane 2: PML/RARα positive PCR products; Lane 3: PML/RARα negative PCR products; Lane 4: blank control. (B) SPR sensorgrams of PCR products: PML/RARα positive PCR products (a), PML/RARα negative PCR products (b), blank control (c).

4. Conclusion

In summary, an enzyme-free and label-free dual amplification SPR biosensing strategy is firstly investigated and applied for ultrasensitive analysis of PML/RARα based on DNA self-assembly aptamer-based hydrogel with SA encapsulation. In comparison with the conventional SPR biosensing strategies based on DNA self-assembly, the developed method can achieve femtomole level detection of PML/RARα with a wide linear range from 100 fM to 10 nM. The excellent performance can be attributed to the admirable signal-to-noise ratio, outputting great amplified SPR signal based on the target-triggered formation of super molecular weight complex on the gold surface with almost negligible background in the absence of target. More importantly, the clinical PCR products of PML/RARα have been successfully identified by the developed biosensing method, demonstrating the practical capability of the method. It is worth pointing out that the proposed biosensor presents a pragmatic platform towards high efficiency detection for a variety of fusion gene in clinical diagnosis.

Acknowledgements

This work was supported by the National Natural Science Foundation of China (81572080, 81371904 and 81702083), the Special Project for Social Livelihood and Technological Innovation of Chongqing (cstc2016shmszx130043).

References

Chou, L.Y., Zagorovsky, K., Chan, W.C., 2014. Nat. Nanotechnol. 9, 148-155.

Chen, Z., Chen, S.J., 1992. Leukemia Lymphoma. 8, 253-260.

Couvreur, P., Vauthier, C., 2006. Pharm. Res. 23, 1417-1450.

Ding, X.J., Cheng, W., Li, Y.J., Wu, J.L., Li, X.M., Cheng, Q., Ding, S.J., 2017. Biosens. Bioelectron. 87, 345-351.

De Thé, H., Chomienne, C., Lanotte, M., Degos, L., Dejean, A., 1990. Nature. 347, 558-561.

Evans, A.C., Thadani, N.N., Suh, J., 2016. J. Control Release. 240, 387-393.

Gao, Y., Wolf, L.K., Georgiadis, R.M., 2006. Nucleic Acids Research. 34, 3370-3377.

Gao, S., Zheng, X., Hu, B., Sun, M., Wu, J., Jiao, B., Wang, L., 2017a. Biosens. Bioelectron. 89, 952-958.

Gao, S., Zheng, X., Wu, J., 2017b. Sensor Actuat B-Chem. 246, 169-174.

He, L., Musick, M.D., Nicewarner, S.R., Salinas, F.G., Benkovic, S.J., Natan, M.J., Keating, C.D., 2000. J. Am. Chem. Soc. 122, 9071-9077.

He, P., Qiao, W.P., Liu, L.J., Zhang, S.S., 2014. Chem. Commun. 50, 10718-10721.

Holtz, J. H., Asher, S.A., 1997. Nature. 389, 829-832.

Hu, Y., Fine, D.H., Tasciotti, E., Bouamrani, A., Ferrari, M., 2011. Wiley Interdiscip. Rev. Nanomed. Nanobiotechnol. 3, 11-32.

Jones, M.R., Seeman, N.C., Mirkin, C.A., 2015. Science. 347, 1260901.

Kouwer, P.H., Koepf, M., Le Sage, V.A., Jaspers, M., van Buul, A.M., Eksteen-Akeroyd, Z.H., Woltinge, T., Schwartz, E., Kitto, H.J., Hoogenboom, R., 2013. Nature. 493, 651-655.

Li, X.M., Wang, Y., Wang, L.L., Wei, Q.L., 2014. Chem. Commun. 50, 5049-5052.

Li, X.M., Cheng, W., Li, D.D., Wu, J.L., Ding, X.J., Cheng, Q., Ding, S.J., 2016a. Biosens. Bioelectron. 80, 98-104.

Li, J.B., Lei, P.H., Ding, S.J., Zhang, Y., Yang, J.R., Cheng, Q., Yan, Y.R., 2016b. Biosens. Bioelectron. 77, 435-441.

Li, J., Mo, L.T., Lu, C.H., Fu, T., Yang, H.H., Tan, W.H., 2016c. Chem. Soc. Rev. 45, 1410-1431.

Liu, R.J., Wang, Q., Li, Q., Yang, X.H., Wang, K.M., Nie, W.Y., 2017. Biosens. Bioelectron. 87, 433-438.

Mastronardi, E., Foster, A., Zhang, X., DeRosa, M.C., 2014. Sensors. 14, 3156-3171.

Nawattanapaiboon, K., Kiatpathomchai, W., Santanirand, P., Vongsakulyanon, A.,

Amarit, R., Somboonkaew, A., Sutapun, B., Srikhirin, T., 2015. Biosens. Bioelectron. 74, 335-340.

Nguyen, H.H., Park, J., Kang, S., Kim, M., 2015. Sensors. 15, 10481-10510.

Sefah, K., Phillips, J.A., Xiong, X., Meng, L., Van Simaeys, D., Chen, H., Martin, J., Tan, W., 2009. Analyst. 134, 1765-1775.

Song, P., Ye, D.K., Zuo, X.L., Li, J., Wang, J.B., Liu, H.J., Hwang, M.T., Chao, J., Su,

S., Wang, L.H., Shi, J.Y., Wang, L.H., Huang, W., Lal, R., Fan, C.H., 2017. Nano Lett. 17, 5193-5198.

Teller, C., Willner, I., 2010. Curr. Opin. Biotechnol. 21, 376-391.

Wang, Q., Li, Q., Yang, X.H., Wang, K.M., Du, S.S., Zhang, H., Nie, Y.J., 2016. Biosens. Bioelectron. 77, 1001-1007.

Xiang, B.B., He, K.Y., Zhu, R., Liu, Z.L., Zeng, S., Huang, Y., Nie, Z., Yao, S.Z., 2016. ACS Appl. Mater. Interfaces. 8, 22801-22807.

Xing, Y., Cheng, E., Yang, Y., Chen, P., Zhang, T., Sun, Y., Yang, Z., Liu, D., 2011. Adv. Mater. 23, 1117-1121.

Yang, H., Liu, H., Kang, H., Tan, W., 2008. J. Am. Chem. Soc. 130, 6320-6321.

Yan, L., Zhu, Z., Zou, Y., Huang, Y., Liu, D., Jia, S., Xu, D., Wu, M., Zhou, Y., Zhou, S., Yang, C.J., 2013. J. Am. Chem. Soc. 135, 3748-3751.

Zhang, L., Lei, J.P., Liu, L., Li, C.F., Ju, H.X., 2013b. Anal. Chem. 85, 11077-11082.

Zhang, Y., Lu, F., Yager, K.G., van der Lelie, D., Gang, O., 2013a. Nat. Nanotechnol. 8, 865-872.

Zhu, Z., Wu, C., Liu, H., Zou, Y., Zhang, X., Kang, H., Yang C.J., Tan, W., 2010. Angew. Chem. Int. Ed. 49, 1052-1056.

Highlights

An enzyme-free and label-free SPR biosensing strategy had been developed for ultrasensitive analysis of PML/RARα based on DNA self-assembly aptamer-based hydrogel with streptavidin encapsulation.

Aptamer-based network hydrogel nanostructure was successfully prepared via sequence-directed hybridization on the gold surface.

The SPR biosensing strategy achieved femtomole level detection of nucleic acids.

The high efficiency biosensing strategy showed excellent practical ability to identify the clinical PCR products of PML/RARα.